

Properties of Voids in the 2dFGRS Galaxy Survey

Anton V. Tikhonov

St. Petersburg State University, St. Petersburg, Russia

avt@gtn.ru, ti@hotmail.ru

ABSTRACT

A method for detecting voids in the galaxy distribution is presented. Using this method, we have identified 732 voids with a radius of the seed sphere $R_{seed} > 4.0h^{-1}$ Mpc in a volume-limited sample of galaxies from the southern part of the 2dFGRS survey. 110 voids with $R_{seed} > 9.0h^{-1}$ Mpc have a positive significance. The mean volume of such voids is $19 \cdot 10^3 h^{-3}$ Mpc³. Voids with $R_{seed} > 9.0h^{-1}$ Mpc occupy 55% of the sample volume. We construct a dependence of the volumes of all the identified voids on their ranks and determine parameters of the galaxy distribution. The dependence of the volume of voids on their rank is consistent with a fractal model (Zipf's power law) of the galaxy distribution with a fractal dimension $D \approx 2.1$ (given the uncertainty in determining the dimension using our method and the results of a correlation analysis) up to scales of $25h^{-1}$ Mpc with the subsequent transition to homogeneity. The directions of the greatest elongations of voids and their ellipticities (oblateness) are determined from the parameters of equivalent ellipsoids. The directions of the greatest void elongations have an enhanced concentration to the directions perpendicular to the line of sight.

PACS numbers : 98.65.Dx

DOI: 10.1134/S1063773706110028

Key words: galaxies, voids, large-scale structure.

1. Introduction

Information about the structuring of the spatial distribution of luminous matter (the form and degree of clustering of galaxies and clusters of galaxies, the characteristic scales of clustering, etc.) characterizes the physical conditions at the formation epoch of the observed inhomogeneities.

The first galaxy redshift surveys revealed that the spatial distribution of galaxies is essentially inhomogeneous: they are gathered in groups and clusters, which, in turn, form a complex network of filaments and walls that are threaded by tunnels and that bound voids (a foamy or cellular structure).

In the early 1980s, it became clear that giant voids in the distribution of galaxies are common in the observable Universe (Einasto et al. 1980; Kirshner et al. 1981), but their significance was understood later. The history of void detection and description was presented by Rood (1988).

Describing the distribution and parameters of voids in the distribution of galaxies is important for understanding the formation conditions of the large-scale structure of the observable Universe and imposes constraints on cosmological model parameters (Peebles 2001; Berlind and Weinberg 2002). CDM models predict a certain amount of matter and, hence, galaxies in voids. However, studies have shown that dwarf galaxies are located in the same structures as normal galaxies (Gottlober et al. 2003; Hoyle and Vogeley (2002) and references therein).

The model of cellular structure allows a void to be defined as a connected region of space with a reduced density of galaxies compared to the regions containing the formations that constitute the large-scale structure (walls, filaments, and clusters) or completely free from galaxies. The methods for analyzing the distributions of void parameters complement the methods for studying the distribution of galaxies; in particular, describing the spectrum of void volumes allows the morphology of the distribution under study to be determined. VPF (Void Probability Function) and UPF (Underdensity Probability Function) are the standard statistical methods that determine high order correlation functions. VPF determines the probability that a sphere of radius r placed in a given distribution will be empty; UPF measures the frequency of spheres with a density contrast $\delta\rho/\rho$ below a certain threshold.

There are several algorithms for identifying voids in a point distribution that do not determine the void shapes a priori. The most developed algorithms are given in the papers by El-Ad and Piran (1997) – the method of nonoverlapping spheres, Aikio and Mahonen (1998) – the method of maxima of the field of distances, Gaite (2005) – the method of Delaunay and Voronoi tessellations, and Shandarin et al. (2006) – using a smoothed density field. Different algorithms provide different lists of voids.

The shapes of voids along with the spectrum of their sizes are of considerable interest. For example, Plionis and Basilakos (2002) analyzed the distributions of void sizes and shapes in the PSCz survey and compared them with artificial distributions obtained using various CDM models.

Hoyle and Vogeley (2004) have already searched the 2dFGRS survey for voids using an algorithm similar to that presented by El-Ad and Piran (1997) and Croton et al. (2004) based on VPF. Using the method of searching for maximum spheres free from galaxies with masses (luminosities) below a certain value, Patiri et al. (2005) determined the statistical parameters of such voids in the distribution of 2dFGRS galaxies.

2. THE METHOD OF SEARCHING FOR VOIDS

The void finder algorithm presented here is similar to the procedure described by El-Ad and Piran (1997) and differs from the approach used by Hoyle and Vogeley (2004).

Here, we searched for voids that were completely free from galaxies (without separating the galaxies into wall and void galaxies), because the procedure for constructing a volume-limited sample leaves only fairly bright galaxies that outline the structure (formed inside massive halos) in the sample.

Our method uses a standard (for a number of related methods) ad hoc parameter (in our case, the parameter k) that defines the size of the tunnel (hole) in the distribution of galaxies into which a given void penetrates during the construction. The method used by Shandarin et al. (2006) is free from such parameters. However, when a smoothed density field is constructed, the void parameters depend on the smoothing length (e.g., in the case of smoothing by a Gaussian filter) and on the threshold density that separates the regions with enhanced and reduced densities. Besides, this approach yields very irregular voids.

The method presented here is fairly simple, flexible, and suitable for searching for voids defined as regions completely free from galaxies.

An orthogonal three-dimensional grid is constructed in the volume of the sample under study to attribute the grid points to a particular void. The voids are identified from large to small ones. First, the sphere with the largest possible radius that fits into the empty (free from galaxies) regions of the galaxy distribution and the geometrical boundaries of the sample is identified. Since the voids are assumed to lie strictly within the geometrical boundaries of the sample, the radius for a given grid point is defined as the minimum of the smallest distance from the given grid point to galaxies and the minimum distance from the point to the boundary.

Inside the sample volume, galaxy-free seed spheres are sequentially searched for (first, the largest sphere is searched for) followed by their expansion through the addition of the spheres whose centers are located within the already fixed part of the void and whose radii

R_{sph} are no less than the radius of the seed sphere multiplied by the coefficient $k = 0.9$ ($R_{sph} > 0.9 \cdot R_{seed}$, where R_{seed} is the radius of the seed sphere). Thus, the spheres added to the void overlap with the region already attributed to the void by more than 30% of their volume. Subsequently, the empty sphere with the largest possible radius is identified again by taking into account the void identified at the previous step (all the grid points attributed to this void are excluded from the analysis), this sphere is then expanded, and so on. The identification of voids continues as long as R_{seed} is larger than a certain value (in our case, $4.0h^{-1}$ Mpc). The radius of the sphere with the volume per galaxy in the volume-limited under study (see below) is $R_{gal} \approx 5.0h^{-1}$ Mpc.

At $k = 0.9$, the voids outline fairly well the regions between galaxies and, at the same time, retain a regular shape, which is convenient when voids are approximated by ellipsoids. At $k = 1$, the voids are strictly spherical. If we decrease k , then the voids begin to penetrate into increasingly small holes and the void shapes become increasingly irregular. At small k , one (the first) void fills most of the sample volume. The coefficient $k = 0.9$ used here is a compromise chosen after the void construction in point distributions with different properties. The voids constructed in this way (at $k = 0.9$) are identified in arbitrarily shaped volumes. On the other hand, the voids are found to be separated from one another and to be fairly thick throughout the volume, which allows them to be approximated by triaxial ellipsoids.

We divided the identified voids into the voids that completely lie within the geometrical boundaries of the sample and the voids that touch the sample boundaries; hence, their volumes are underestimated and their shapes are distorted by the boundary effect.

3. THE DATA

The second release of the 2dFGRS galaxy and quasar survey (Colless et al. 2001, 2003) includes ~ 250000 galaxies and up to 25 000 quasars. A multiobject spectrograph with a 2° field of view capable of taking 400 spectra in a single exposure was used to determine the redshifts. The APM ($b_j < 20.5$) photometric catalog formed the basis for the survey. All of the galaxies with Galactic extinction-corrected apparent magnitudes b_j in the range $14.5 < b_j < 19.5$ were selected for the 2dFGRS survey. The main region in the sky covered by the 2dFGRS survey consists of two strips: 80° in right ascension and 15° in declination near the South Galactic Pole and 75° in right ascension and 10° in declination in the Northern Galactic Hemisphere. Additionally, galaxies in 99 randomly located fields in the high-latitude part of the South Galactic Hemisphere were imaged for the survey. The survey covers ~ 2000 square degrees and has a median depth of $z = 0.11$ for galaxies with $b_j < 19.45$. In this paper, we use a sample from the southern part of 2dFGRS and consider

galaxies with a redshift quality parameter (z) $quality \geq 3$. The boundaries of the sample are: $21.84^h < \alpha < 23.44^h$, $-35^\circ < \delta < -24^\circ$, and $0.02 < z < 0.121$. At $z_{max} = 0.121$, the volume-limited sample contains the largest number (7219) of galaxies for these angle boundaries. In such a sample, all galaxies with absolute magnitudes $M_{abs} < -19.92$ are observable from any point of the sample with apparent magnitudes $b_j < 19.2$. To estimate the absolute magnitudes of galaxies, we calculated the combined evolutionary correction $e(z)$ and the correction for the shift of the range of the galaxies radiation to the longer wavelengths (the $K(z)$ correction) used to calculate the luminosity function for 2dFGRS galaxies (Norberg et al. 2002): $K(z) + e(z) = (z + 6 \cdot z^2)/(1 + 20 \cdot z^3)$. To determine the metric distances from the redshift using a formula given, for example, in Hogg et al. (1999), we used the Hubble parameter $H_0 = 65 \text{ km s}^{-1} \text{ Mpc}^{-1}$ ($h = H/H_0$, where H is the true value of the Hubble constant) and the density parameters $\Omega_\Lambda = 0.7$, $\Omega_0 = 0.3$. In such a cosmology, $z_{max} = 0.121$ corresponds to a distance of $542.54h^{-1} \text{ Mpc}$.

4. IDENTIFIED VOIDS

We identified a total of 732 voids with $R_{seed} > 4h^{-1} \text{ Mpc}$ in the work sample using the algorithm described above.

The configuration of voids and their volumes to some extent depend on the chosen step of the three dimensional grid. In the presented implementation of the algorithm, we chose the grid step to be $Step \approx 1.0 \text{ Mpc}$. The void volumes were estimated as $Step^3 \times N$, where N is the number of grid points inside a given void. The volume per galaxy in our sample is $513h^{-3} \text{ Mpc}^3$. The largest found void occupies a volume of $85595h^{-3} \text{ Mpc}^3$. The radius of the first (largest) seed (initial) sphere is $R_{seed}^1 = 21.3h^{-1} \text{ Mpc}$. In Fig.1, the void volume is plotted against the radii R_{seed} of the seed spheres. As expected, the scatter of volumes increases with R_{seed} .

We determined the significance of voids by comparing the identified voids with the list of voids obtained using the same algorithm in a random sample with the same mean density. The significance is $P(r) = 1 - N_{random}(r)/N_{survey}(r)$, where $N_{survey}(r)$ is the number of seed spheres of voids with radii $R_{seed} > r$ identified in the 2dFGRS sample and $N_{random}(r)$ is the number of seed spheres identified in a homogeneous distribution within the same boundaries and with the same mean density as that for the galaxy sample (Fig. 2). 110 voids of the 2dFGRS sample with radii $R_{seed} > 9h^{-1} \text{ Mpc}$ have a positive significance; 23 of them do not touch the boundaries. All the significant voids touch at least one galaxy in the process of construction. Figure 3 shows the projection of the distribution of galaxies with $-32^\circ < \delta < -27^\circ$ and the centers of 110 voids with $R_{seed} > 9h^{-1} \text{ Mpc}$.

The mean volume of the voids with significance $R_{seed} > 9h^{-1}$ Mpc is $18666h^{-3}$ Mpc³. The ratio of the total volume of the seed spheres to the total volume of the voids ($R_{seed} > 9h^{-1}$ Mpc) is 0.31. On average, the seed sphere occupies 0.32 of the volume of the void grown from it for significant voids. Figure 4 shows the distribution of void volumes. A nearly power-law decrease in the number of voids with increasing volume is observed.

The voids identified using the algorithm presented here with $R_{seed} > 9h^{-1}$ Mpc occupy 55% of the sample volume.

5. VOLUME STATISTICS. PARAMETERS OF THE GALAXY DISTRIBUTION

The distribution of galaxies (the behavior of the density with distance) is known to obey a power law on small scales. This is occasionally interpreted as fractality, self-similarity in a certain interval of scales (up to $20-30h^{-1}$ Mpc). Fractal methods yield a fractal dimension of ~ 2 (Coleman and Pietronero 1992; Baryshev and Teerikopi 2005; Tikhonov 2005). Gaite and Manrubia (2002) showed that the fractal dimension could be derived from the distribution of void volumes in a fractal structure: Zipfs power-law (Zipfs 1949) dependence of the volume on rank (the largest void has rank 1, the next void has rank 2, etc.) is valid for the volumes of the voids identified in a three-dimensional fractal distribution: $V(Rank) \propto Rank^{-z_f}$, $z_f = 3/D$, where D is the fractal dimension of the distribution.

Gaite and Manrubia (2002) found no power-law dependence using some of the void catalogs and suggested that Zipfs law was not observed in the cases considered because of the algorithms used for void identification. Artificial fractal distributions, including the distribution obtained using the Cantor dust algorithm also known as a β -cascade (Paladin and Vulpiani 1987), revealed that the algorithm presented in this paper overestimates the fractal dimension D by $0.1 - 0.2$ at $D \geq 2$ and poorly estimates it at $D < 2$ ($D > 2$ is a fundamental limitation for estimating the dimension using Zipfs law (Gaite 2006)); a well-defined power-law dependence is observed in all cases. In Fig.5, the volumes of all 732 voids identified in the 2dFGRS sample is plotted against their ranks. The bend of the dependence at the highest ranks (smallest volumes) is due to the limitation on the radius of the seed sphere from below. The dependence in Fig.5 can be interpreted in terms of Zipfs law from small volumes to $V_{break} \sim 10^4 h^{-3}$ Mpc³. After the smooth break, the slope of the dependence toward the larger volumes (lower ranks) becomes less than unity, which rules out the fractal interpretation (Gaite and Manrubia 2002). Gaite (2005) interpreted this behavior of the dependence as a manifestation of the transition to homogeneity in the given distribution. The effective diameter (the diameter of a sphere with the same volume)

for V_{break} is $\sim 26h^{-1}$ Mpc. This diameter virtually coincides with the scale on which the correlation gamma-function deviates significantly from a power law (Tikhonov et al. 2000; Tikhonov 2005). The slope before the break (at high ranks) is $z_f \approx 1.4$, which corresponds to a fractal dimension of $D = 3/z_f \approx 2.14$ and also agrees with the results of the correlation analysis (e.g., of the 2dFGRS survey (Tikhonov 2005)).

6. VOID SHAPES

Once we compiled the list of voids (attributed three-dimensional grid points to a particular void), we determined the void centers and calculated the moments of inertia of the bodies formed by the voids. We analyzed the void shapes using the parameters of their equivalent ellipsoids. We constructed the 3×3 matrix of moments of inertia I_{ij} and found its eigenvalues λ_i , which are equal to the principal moments of inertia, from the condition $\det(I_{ij} - \lambda \cdot E) = 0$ (where E is a 3×3 unit matrix); these principal moments of inertia were used to determine the semiaxes of the equivalent triaxial ellipsoid. The eigenvectors of the matrix I_{ij} give the directions of the semiaxes. The direction of the greatest void elongation coincides with the direction of the major axis of the equivalent ellipsoid. The distribution of the directions of void elongations is not quite homogeneous (Fig. 6): we can note a crowding toward the directions perpendicular to the line of sight (especially of the major axes of the voids that do not touch the boundaries). No void elongation along the line of sight is observed. The ellipticity (oblateness) of voids was defined as $\epsilon = 1 - c/a$, where a and c are the semimajor and semiminor axes, respectively. 37 and 8 voids with $R_{seed} > 9.0h^{-1}$ Mpc have $\epsilon > 0.4$ and $\epsilon < 0.15$, respectively; the largest ellipticity is $\epsilon = 0.61$. The voids are distributed in ellipticity rather homogeneously (Fig. 7).

7. CONCLUSIONS

In this paper, we presented an algorithm for identifying voids without prior determination of their shapes. We identified 110 significant voids with radii of the seed spheres $R_{seed} > 9.0h^{-1}$ Mpc in the southern part of the volume-limited sample from the 2dFGRS galaxy survey. These voids occupy 55% of the sample volume. The table gives parameters of the nine largest voids with volumes larger than $40 \cdot 10^3 h^{-3}$ Mpc³ (Fig. 8). The mean effective radius of voids, $16.46h^{-1}$ Mpc, is considerably smaller than that obtained by Hoyle and Vogeley (2004) the algorithm presented here identifies voids of smaller volumes, because the galaxies are not divided into wall and void galaxies (we used all of the galaxies included in the work sample). The distribution of the directions of the major axes of voids is not

quite homogeneous. There is no tendency for them to be grouped near the line-of-sight direction, but there is a crowding of the directions of the major axes of voids near the direction perpendicular to the line of sight; this can be observed in redshift space if the voids contract homogeneously in the comoving coordinates during the cosmological evolution (Ryden and Melott 1996). No systematic trends are observed in the distribution of void ellipticities (oblateness). The dependence of the volumes of voids on their ranks exhibits a power-law portion at high ranks that can be interpreted in terms of Zipf's law with a fractal dimension of $D \approx 2.1$ of the galaxy distribution. The behavior of this dependence at lower ranks (at void volumes larger than $10^4 h^{-3} \text{Mpc}^3$), which is indicative of the transition to a homogeneous distribution from a scale of $\sim 25h^{-1}$, is consistent with the results of the correlation analysis of the 2dFGRS sample.

8. ACKNOWLEDGMENTS

I wish to thank D. Makarov and J. Gaite for helpful discussions and the Administration of St.-Petersburg for support (grant PD05-1.9-117).

9. REFERENCES

1. J. Aikio and P. Mahonen, *Astrophys. J.* 497, 534 (1998).
2. Y. Barishev and P. Teerikorpi, *astro-ph/0505185* (2005).
3. A. Berlind and D. H. Weinberg, *Astrophys. J.* 575, 587 (2002).
4. P. H. Coleman and L. Pietronero, *Phys. Rep.* 213, 311 (1992).
5. M. Colles, G. Dalton, S. Maddox, et al. (The 2dFGRS Team), *Mon. Not. R. Astron. Soc.* 328, 1039 (2001).
6. M. Colles, B. Peterson, C. Jackson, et al. (The 2dFGRS Team) *astro-ph/0306581* (2003).
7. D. J. Croton, M. Colles, E. Gaztanaga, et al., *Mon. Not. R. Astron. Soc.* 352, 828 (2004); *astro-ph/0401406* (2004).
8. J. Einasto, M. Joeveer, and E. Saar, *Mon. Not. R. Astron. Soc.* 193, 353 (1980).
9. H. El-Ad and T. Piran, *Astrophys. J.* 491, 421 (1997).
10. J. Gaite, *astro-ph/0510328* (2005).

11. J. Gaite, private communication (2006).
12. J. Gaite and S. C. Manrubia, *Mon. Not. R. Astron. Soc.* 335, 977 (2002); astro-ph/0205188 (2002).
13. S. Gottlober, E. L. Locas, A. Klypin, and Y. Hoffman, astro-ph/0305393 (2003).
14. D.W. Hogg, astro-ph/9905116 (1999).
15. F. Hoyle and M. S. Vogeley, *Astrophys. J.* 566, 641 (2002); astro-ph/0109357.
16. F. Hoyle and M. S. Vogeley, *Astrophys. J.* 607, 751 (2004); astro-ph/0312533.
17. R. P. Kirshner, A. Jr. Oemler, P. L. Schechter, and S. A. Shectman, *Astrophys. J.* 248, L57 (1981).
18. P. Norberg, S. Cole, C. M. Baugh, et al., *Mon. Not. R. Astron. Soc.* 336, 907 (2002); astro-ph/0111011 (2001).
19. G. Paladin and A. Vulpiani, *Phys. Rep.* 156, 147 (1987).
20. S. G. Patiri, J. Betancort-Rijo, F. Prada, et al., submitted to *Mon. Not. R. Astron. Soc.*; astro-ph/0506668 (2005).
21. P. J. E. Peebles, *Astrophys. J.* 557, 495 (2001).
22. M. Plionis and S. Basilakos, *Mon. Not. R. Astron. Soc.* 330, 399 (2002).
23. H. J. Rood, *Ann. Rev. Astron. Astrophys.* 26, 245 (1988).
24. B. S. Ryden and A. L. Melott, *Astrophys. J.* 470, 160 (1996); astro-ph/9510108.
25. A. V. Tikhonov, *Pisma Astron. Zh.* 31, 883 (2005) [*Astron. Lett.* 31, 787 (2005)].
26. A. V. Tikhonov, D. I. Makarov, and A. I. Kopylov, *Bull. Spec. Aastrofiz.Obs., Russ. Akad. Sci.* 50, 39 (2000); astro-ph/0106276 (2001).
27. S. Shandarin, H. A. Feldman, K. Heitmann, and S. Habib, *Mon. Not. R. Astron. Soc.* 367, 1629 (2006).
28. G. K. Zipf, *Human Behavior and the Principle of Least Effort* (Addison-Wesley, Massachusetts, 1949).

Table 1: Parameters and locations of the nine largest voids in the 2dFGRS survey

N	R_{seed}	Volume	Void centers			Ellipsoid axes			ϵ	Direction a	
			r	α	δ	a	b	c		α	δ
	(Mpc*)	(Mpc ³)	(Mpc)	(hours)	(deg.)	(Mpc)	(Mpc)	(Mpc)		(hours)	(deg.)
1**	21.33	68696	494.325	22.684	-27.966	27.87	25.60	23.08	0.17	8.99	-82.6
2	20.19	85595	276.871	23.032	-28.116	38.88	24.43	21.72	0.44	9.21	-31.3
3**	19.99	57727	432.158	22.622	-30.581	27.77	22.81	21.85	0.21	6.68	-76.2
4	19.25	66112	463.606	22.371	-27.317	34.49	21.99	20.95	0.39	0.46	19.6
5	19.24	59241	510.441	22.038	-26.597	27.26	25.42	20.57	0.25	5.81	-50.5
6	19.05	44355	499.752	22.147	-32.629	24.39	21.30	20.45	0.16	11.74	16.5
7	18.96	66518	317.730	22.465	-28.069	31.83	23.64	21.45	0.33	1.22	-55.0
8	18.45	46601	206.704	22.351	-29.214	25.00	22.96	19.50	0.22	7.91	-49.3
20	14.25	41221	448.997	22.020	-26.783	27.99	20.88	17.41	0.38	11.52	45.0

Note. N is the numbering that corresponds to the order of void construction; the void centers are the equatorial coordinates (α_{2000} , δ_{2000}) of the void centers determined as the centers of mass of the figures identified by the algorithm; (ϵ) is the ellipticity; Direction a is the direction of the major axis a of the equivalent ellipsoid.

* — In what follows, the units of h^{-1} are used in the table.

** — The voids do not touch the sample boundaries.

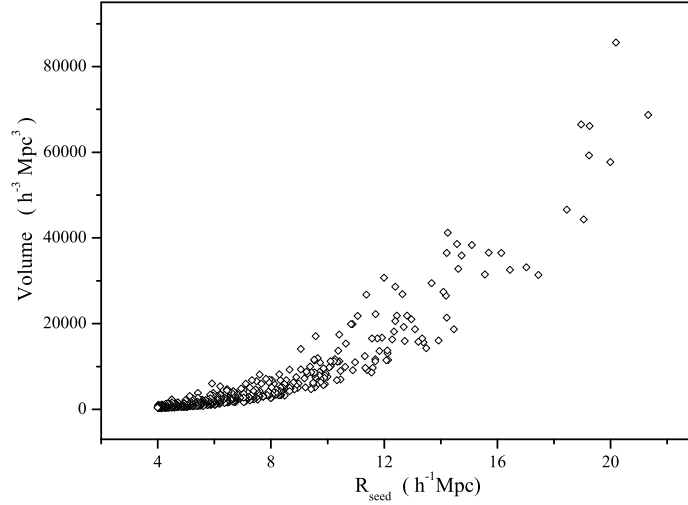


Fig. 1.— Distribution of void volumes vs. radii R_{seed} of the seed spheres of these voids.

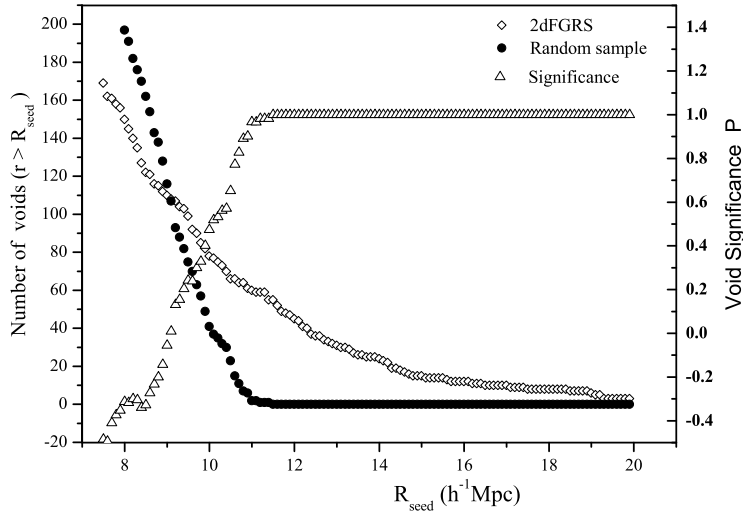


Fig. 2.— Number of voids with the radii of the seed spheres larger than R_{seed} in the 2dFGRS sample (diamonds) and the random sample (circles). The triangles indicate the statistical significance of voids P as a function of R_{seed} .

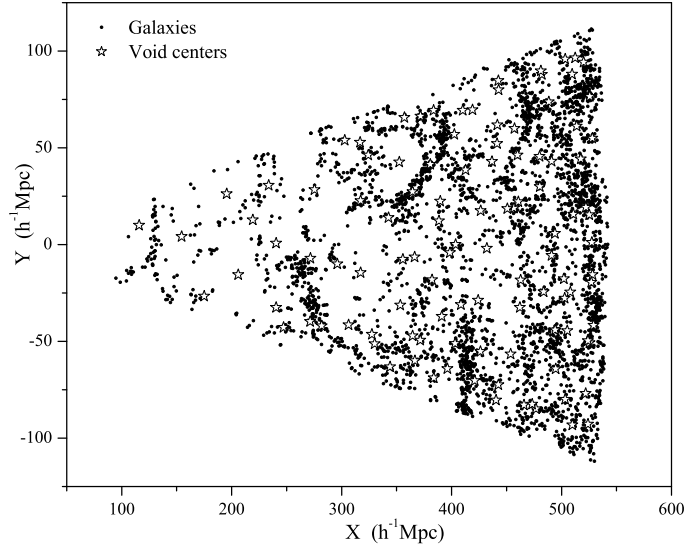


Fig. 3.— Projection of the distribution of the centers of 110 voids with $R_{seed} > 9h^{-1}$ Mpc (asterisks) and the distribution of galaxies from the 2dFGRS work sample (dots) with $-32^\circ < \delta < -27^\circ$.

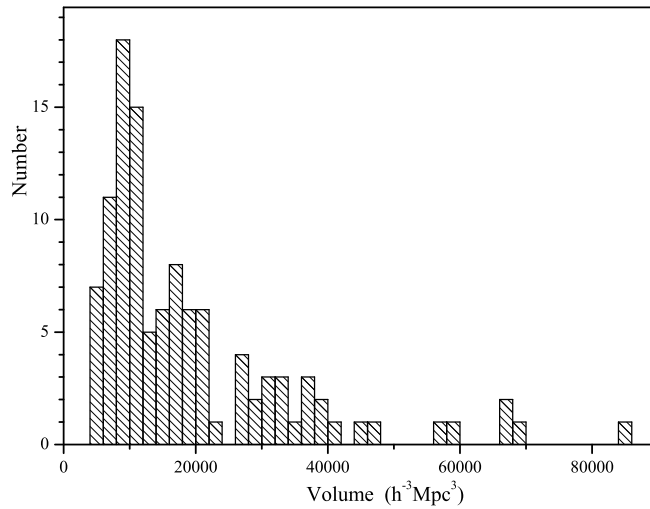


Fig. 4.— Distribution (histogram) of void volumes with $R_{seed} > 9h^{-1}$ Mpc.

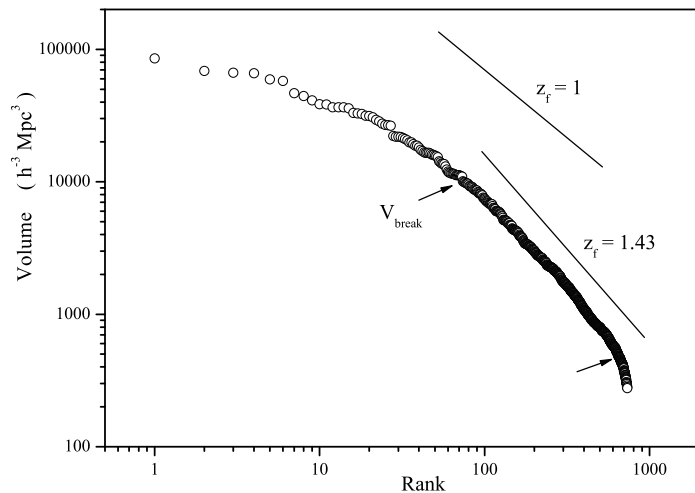


Fig. 5.— Void volume vs. void rank. V_{break} corresponds to the break in the dependence. The arrows indicate the range of the linear fit.

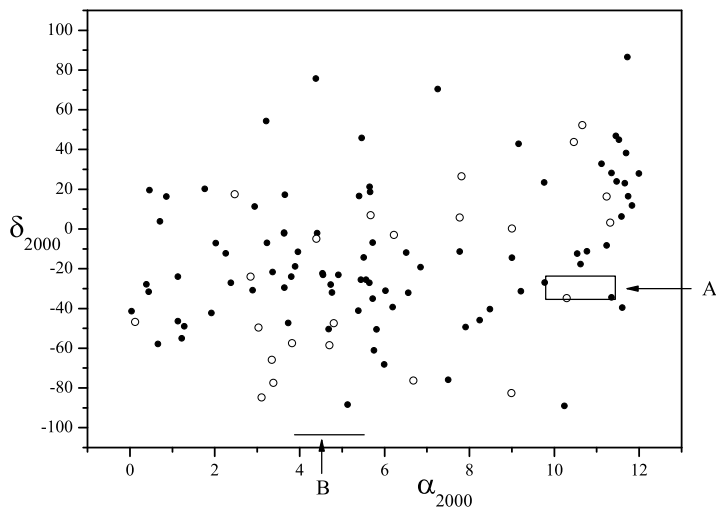


Fig. 6.— Directions of the greatest elongations of voids with $R_{seed} > 9h^{-1}$ Mpc (transferred to the hemisphere $0^h < \alpha < 12^h$). The open circles indicate the directions of 23 voids that do not touch the sample boundaries; the filled circles indicate the directions of the voids that touch the sample boundaries. A – the rectangle of line-of-sight directions for the 2dFGRS sample used here; B – the α range of directions perpendicular to the line of sight.

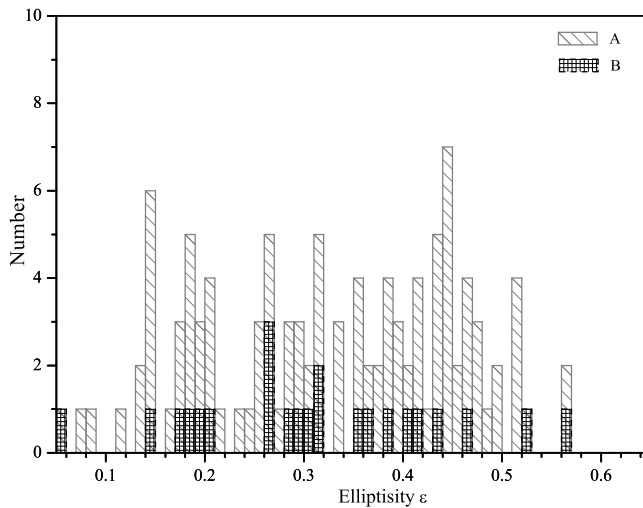


Fig. 7.— Distribution (histogram) of voids ellipticities: A – all voids with $R_{seed} > 9.0h^{-1}$ Mpc and B – voids with $R_{seed} > 9.0h^{-1}$ Mpc that do not touch the boundaries.

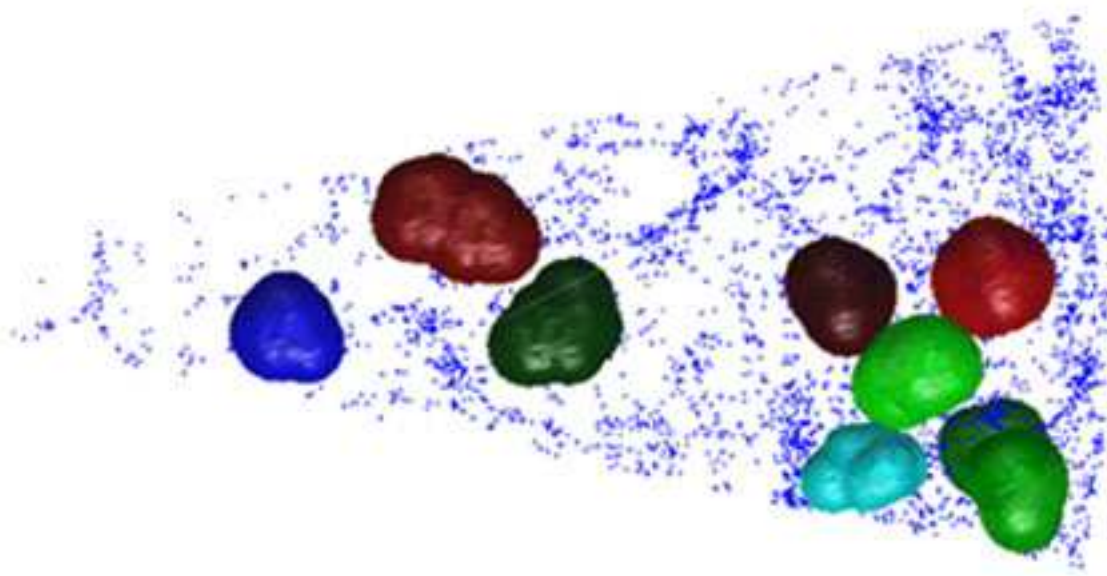


Fig. 8.— Nine largest identified voids and galaxies of the 2dFGRS work sample with $-32^\circ < \delta < -27^\circ$.